J Mater Sci (2008) 43:4316–4322
DOI 10.1007/s10853-008-2633-y

Effect of microstructure on the mechanical properties of PAN-based carbon fibers during high-temperature graphitization

Fujie Liu · Haojing Wang · Linbing Xue · Lidong Fan · Zhenping Zhu

Received: 15 January 2008 / Accepted: 4 April 2008 / Published online: 17 April 2008

Abstract The change of microstructure of PAN-based carbon fibers has been studied as a function of heat-treatment temperature (1,800–2,800 °C, stretching 0%) by Raman spectroscopy and X-ray diffraction. With increasing heat-treatment temperature, both the crystallite size (L_a, L_c) and the degree of preferred orientation (g) increase, while the crystallite interlayer spacing (d_{002}) decreases. The values of both R_s and R_c decrease, while R_s decreases more quickly. It implies that the degrees of skin-core of the carbon fibers increase. The relationship between mechanical properties and microstructure of the variants is also explored in detail.

Introduction

Carbon fibers are, perhaps, the most successful new carbon product to be commercialized in the past 45 years. Their high strength and stiffness, combined with lightweight, make these fibers attractive for high-volume applications ranging from sporting goods to aircraft structures. Since the properties of carbon fibers directly depend on the structure, the control of structure and the relationship between the structure and properties during graphitization have been extensively studied by a number of researchers [1–4].

Skin-core structure affects the properties of carbon fibers. Investigations have taken place into the microstructural differences between the skin and core regions of carbon fibers. Wicks and Coyle [5] observed a two-phase structure with almost perfectly oriented material close to the surface and poorly oriented material in the center of PAN-based fibers. Dieter et al. [6] found that the fiber structural parameters in dependence on the normalized local position of the carbon fiber, and with heat-treatment temperature increasing, the increase in size and orientation of the crystallites is significantly higher in the skin as compared to the core.

Raman spectroscopy combines a prominent surface selectivity (the depth of analysis has been estimated to be a few hundred angstrom) with an exceptional sensitivity to the degree of structural order. So it is one of the most informative methods for investigation of the structural perfection of carbon fibers [7–12]. However, as we have learned that most researchers used Raman microscopy to study the fiber's surface structure and the study of inner structure is rarely seen. This present study is concerned with the change of microstructure, especially the skin-core structure of PAN-based carbon fibers under different heat-treatment temperature mainly by Raman spectroscopy and X-ray diffraction. In the end, the relationships between microstructures and mechanical properties are also discussed in detail.

Experimental

Materials

All experiments in this study were performed on PAN-based carbon fibers made by our lab, with typical values of 218 and 3.56 GPa for tensile modulus and tensile strength,

F. Liu (✉) · H. Wang · L. Xue · L. Fan · Z. Zhu
Institute of Coal Chemistry, Chinese Academy of Science, Taiyuan 030001, People's Republic of China
e-mail: fjie520@163.com

F. Liu
Graduate School of the Chinese Academy of Sciences, Beijing 100039, People's Republic of China

respectively. The density of as-received carbon fibers is 1.76×10^3 kg/m^3.

Characterization

The carbon fibers underwent continuous graphitization processing in a graphitization furnace with a hot-zone length of 0.22 m. One bundle of carbon fibers went through the furnace at one time. The experiments were carried out in argon atmosphere and the residence time in high-temperature zone was about 20 s. Heat-treatment temperature was conducted at temperatures ranging from 1,800 to 2,800 °C.

Mechanical properties were tested in the form of tows and measured by AG-1 type universal material tester (Shimadzu Co., Ltd., Japan), in which crosshead speed was 3.33×10^{-4} m/s and gauge length was 0.2 m, 10 filaments were tested, and the average value was reported.

The microstructure was analyzed using a X-ray diffraction analyzer (Rigaku D/max-rA, CuKα, 1.5148×10^{-10} m, 40 kV, 60 mA) using a fiber specimen attachment. Fiber bundles were arranged parallel to each other and examined in symmetric transmission. Measurements were made by performing equatorial scan (perpendicular to the fiber axis), meridian scan (parallel to the fiber axis), as well as azimuthal scan (rotating the fibers in the attachment) at the fixed Bragg position, respectively. Silicon was used as a standard for peak position and broadening correction. The diffraction scan curve was fitted with Gaussian or Lorentzian to get peak position and peak widths, and the structure parameters of all samples were obtained as follows: the 002 peak from equatorial scan was used to estimate the value of the average interlayer spacing, d_{002}, and the apparent crystallite thickness, L_c, whereas the 100 peak from meridian scan was used for the apparent layer-plane length parallel to the fiber axis, L_a. The value of d_{002} was calculated using Bragg's law, and the crystallite size L_c and L_a were calculated using Scherrer's formula:

$$d_{002} = \frac{\lambda}{2 \sin \theta}; L = \frac{K\lambda}{\beta \cos \theta}$$

where θ is the scattering angle, λ is the wavelength of the X-rays used, and β is the full width at half maximum intensity (FWHM). The form factor K is 0.89 for L_c and 1.84 for L_a, respectively [13, 14].

The degree of preferred orientation of graphite layer planes (g) parallel to the fiber axis was obtained from azimuthal scan at the fixed Bragg position of the 002 reflection. The g was calculated by using the following formula:

$$g = \frac{(90^\circ - Z)}{90^\circ} \times 100\%$$

where Z is the full width at half maximum intensity of the azimuth.

The Raman scattering measurements were performed from a Raman spectrometer (Renishow, HR800) at room temperature, using a 5.145×10^{-7} m line of an argon ion laser as the incident radiation. The Raman-scattered light was dispersed by an optical grid and detected by a CCD camera, and the instrument was calibrated against the Stokes Raman signal of pure Si at 520 cm^{-1} using a silicon wafer. The Raman spectrometer was operated in the continuous scanning mode with laser beam powers of 4 mW and exposure times of 30 s. The laser spot diameter reaching the fiber surface was about 2×10^{-6} m. Instrument control and spectra analysis were performed with the software packages Renishow WiRE and the spectral resolution was about 2 cm^{-1}.

Results and discussion

Mechanical properties changes

Figure 1 shows the effect of graphitization temperature on tensile strength and tensile modulus of PAN-based carbon fibers. As shown in Fig. 1, the tensile strength decreases linearly (Fig. 1a), while the tensile modulus invariably increases (Fig. 1b) with increasing heat-treatment temperature. The reasons for the change of tensile strength and tensile modulus will be discussed in the following sections.

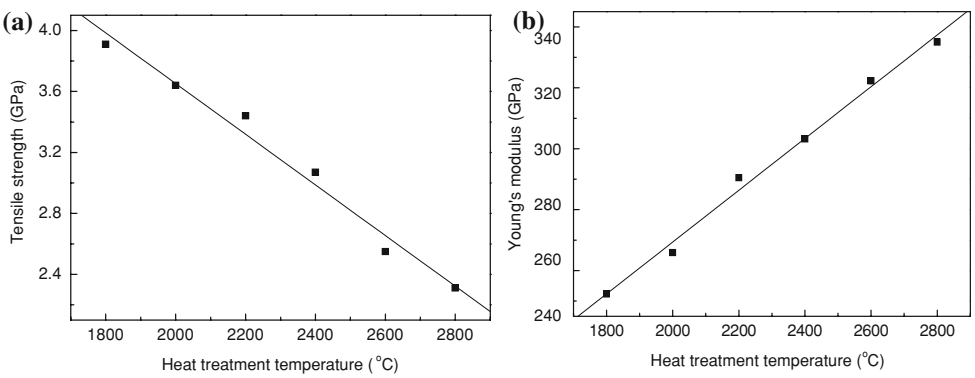

Fig. 1 The tensile strength (**a**) and tensile modulus (**b**) of PAN-based carbon fibers as a function of heat-treatment temperature from 1,800 to 2,800 °C

X-ray diffraction analysis

Figure 2 shows the XRD patterns of as-reserved carbon fibers heat-treated to 2,800 °C, which are observed from equatorial, meridian, and azimuthal scans, respectively. There is an evident difference between equatorial and meridian scans. The appearance of 100 and 110 peaks and no 002 peak in the meridian scans indicate the preferred orientation of layer plane of crystallite along the fiber axis. In addition, when heat-treated to 2,800 °C, 101 or 112 peaks of the XRD pattern for the three-dimensional graphite structure do not appear.

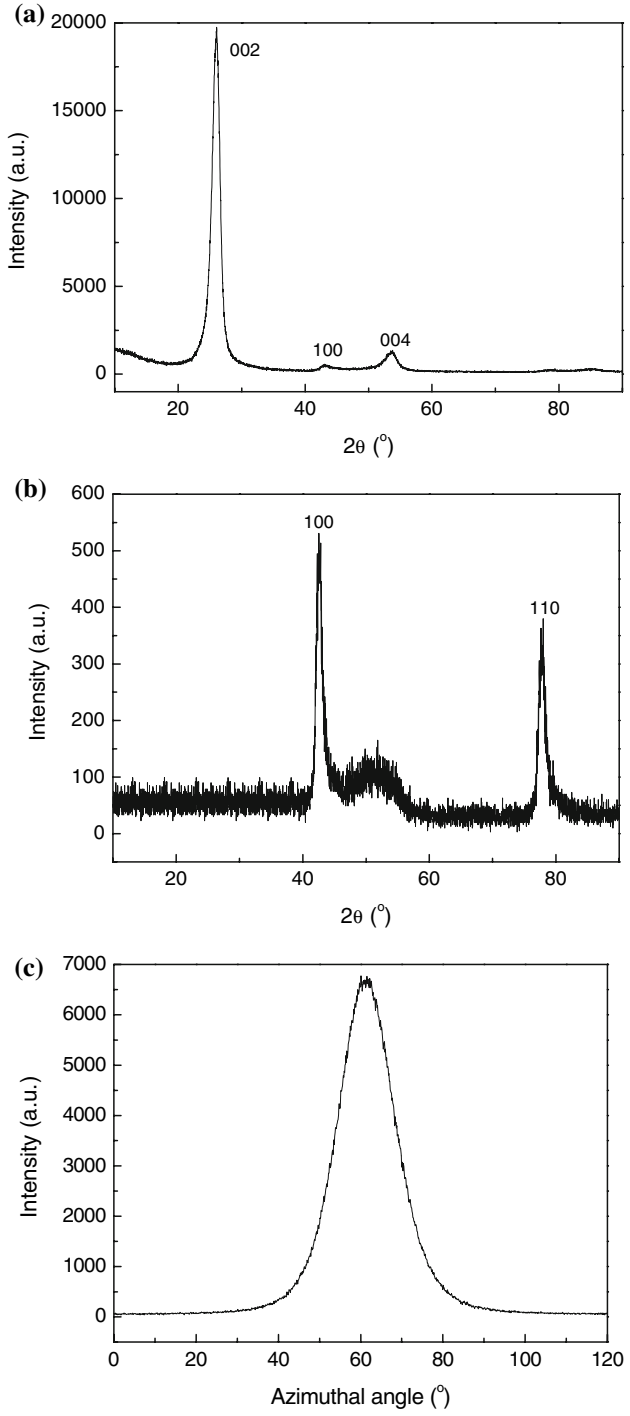

Fig. 2 X-ray diffraction patterns of as-received fibers heat-treated to 2,800 °C: (**a**) equatorial scan, (**b**) meridian scan, and (**c**) azimuthal scan

Crystallite thickness, L_c, and crystallite length, L_a, are plotted as a function of heat-treatment temperature in Fig. 3a, b for the PAN-based carbon fibers used. The results show an increase in L_c and L_a with increasing heat-treatment temperature, while L_a increases more quickly. This graphitization behavior could be due to the increasing degree of graphitizability of the fibers caused by molecular mobility and the structural rearrangement with increasing heat-treatment temperature.

Figure 4 shows the crystallite interlayer spacing, d_{002}, of PAN-based carbon fibers as a function of heat-treatment temperature from 1,800 to 2,800 °C. The results show a decrease in d_{002} with increasing heat-treatment temperature. By heat-treatment temperature at 2,800 °C, d_{002} contracts by ca 2.50% from that of 1,800 °C. The value of d_{002} of carbon fibers heat-treated at 2,800 °C is 3.435×10^{-10} m, which is also much larger than that of highly oriented pyrolytic graphite (HOPG) (3.354×10^{-10} m). It implies that the PAN-based carbon fibers are hard to absolutely graphitize.

Figure 5 shows the degree of crystallite preferred orientation, g, of PAN-based carbon fibers as a function of heat-treatment temperature from 1,800 to 2,800 °C. It is noted that a degree of crystallite preferred orientation of 100% represents perfect alignment of the graphene planes in the fiber axis direction. Data indicate that the crystallite preferred orientation degree is fairly small before heat treatment but increases as heat-treatment temperature increases. By heat-treatment temperature at 2,800 °C, the value of g reaches 84%. However, compared with the highly oriented pyrolytic graphite ($g > 97\%$), the PAN-based carbon fibers only have lower degree of preferred orientation even after heat treatment at 2,800 °C.

Raman spectroscopy analysis

Figure 6 shows the Raman spectra from the surface of PAN-based carbon fibers with heat-treatment temperature ranging from 1,800 to 2,800 °C. With increasing heat-treatment temperature, in the first order spectrum (1,000–2,000 cm^{-1}), the carbon fibers show an increase in the Raman intensity and a decrease in the line width of the graphite Raman 1,580 cm^{-1} band (G band) and the disorder-induced 1,360 cm^{-1} band (D band). After heat treatment at 2,000 °C, another peak at about 1,620 cm^{-1} (D2 band) turns up, which can be observed as a shoulder on the G band. The peak at 1,620 cm^{-1} is due predominantly to midzone phonons, which have energies corresponding to

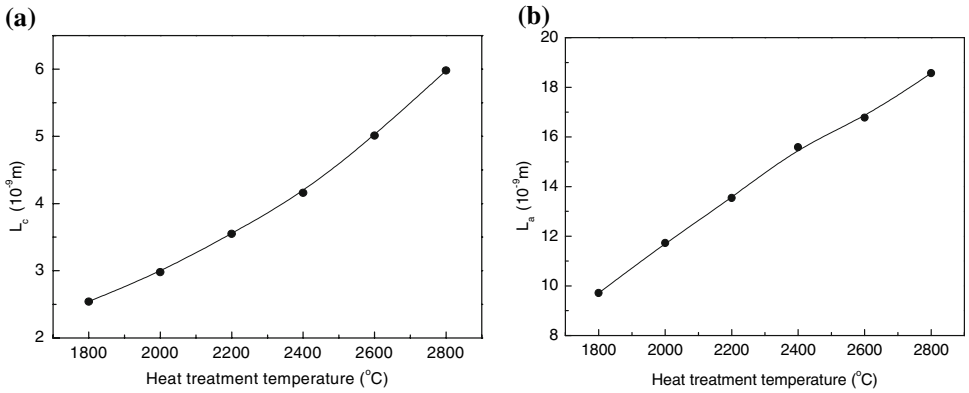

Fig. 3 Crystallite thickness, L_c (**a**), and crystallite length, L_a (**b**), of PAN-based carbon fibers as a function of heat-treatment temperature from 1,800 to 2,800 °C

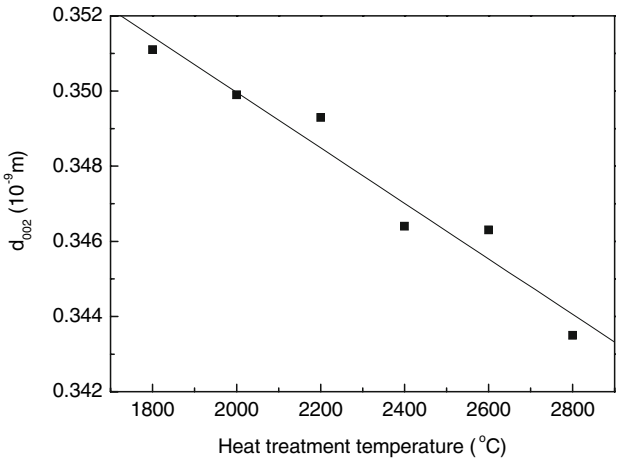

Fig. 4 Crystallite interlayer spacing, d_{002}, of PAN-based carbon fibers as a function of heat-treatment temperature from 1,800 to 2,800 °C

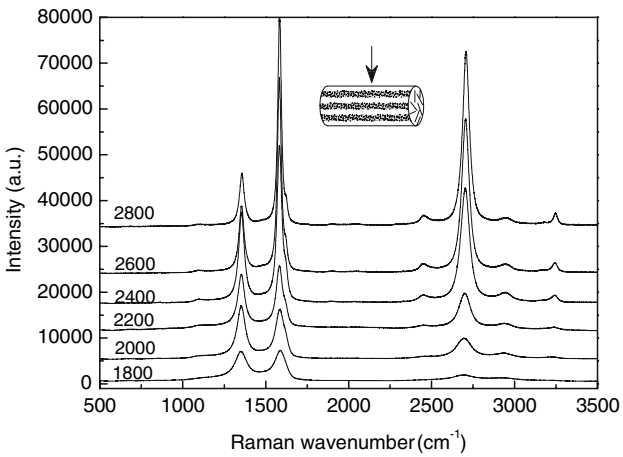

Fig. 6 Raman spectra taken from the surface of PAN-based carbon fibers as a function of heat-treatment temperature from 1,800 to 2,800 °C

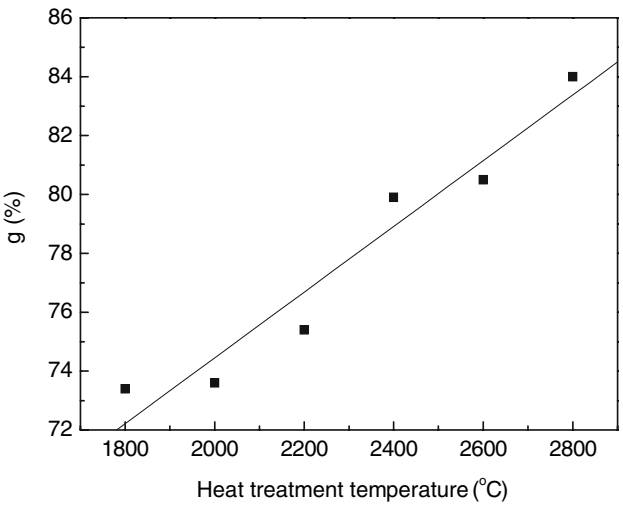

Fig. 5 The degree of crystallite preferred orientation, g, of PAN-based carbon fibers as a function of heat-treatment temperature from 1,800 to 2,800 °C

peaks in the density of phonon modes [15]. At the same time, in the second order spectrum (2,000–3,500 cm^{-1}), the peak at about 2,700 cm^{-1} appears, which can be attributed to the first overtone of the D band (2 * D) [16, 17]. After heat treatment at 2,400 °C, in the second order spectra, three weak characteristic bands appear at about 2,450, 2,950, and 3,240 cm^{-1}, respectively. The band at 2,450 cm^{-1} can be attributed to the Raman-active first overtone of a Raman-inactive graphitic lattice vibration mode at ~1,220 cm^{-1} [17, 18]. The band at 2,950 cm^{-1} can be equaled the sum of the D and G bands. The band at 3,240 cm^{-1} can be assigned to the first overtone of the D2 band (2 * D2) [17]. These phenomena are associated with the development of graphite microcrystalities in PAN-based carbon fibers with heat-treatment temperature more than 2,000 °C.

Figure 7 shows the Raman spectra from the core of PAN-based carbon fibers with heat-treatment temperature ranging from 1,800 to 2,800 °C. These results are very similar to those from the surface. The difference between the surface and the core of the carbon fibers of the Raman spectra is that, with increasing heat-treatment temperature, the intensity of the bands changes more slowly in the core.

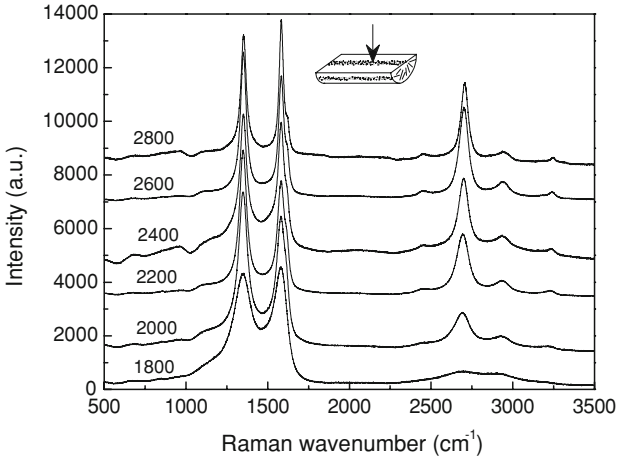

Fig. 7 Raman spectra taken from the core of PAN-based carbon fibers as a function of heat-treatment temperature from 1,800 to 2,800 °C

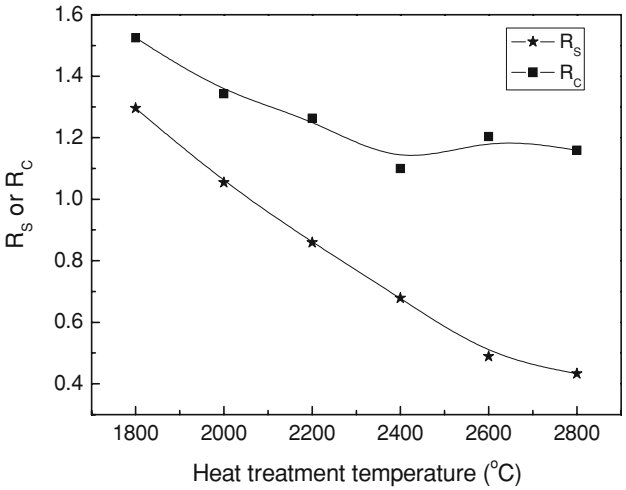

Fig. 8 Plots of the relative intensity, R_s (surface) and R_c (core), of PAN-based carbon fibers as a function of heat-treatment temperature from 1,800 to 2,800 °C

It implies that the effect of heat-treatment temperature to the graphitic degree of carbon fibers core is smaller than that of the carbon fibers surface. The quantitative explanation will be given as follows.

The degree of structural disorder of the fibers can be characterized by the ratio of integrated intensity of the disorder-induced band $(I_{D(1360\ \mathrm{cm}^{-1})})$ to the Raman-allowed band $(I_{G(1580\ \mathrm{cm}^{-1})})$, which describes the amount of disorganized material in the material, and the formula as the following:

$$R = \frac{I_{D(1360\ \mathrm{cm}^{-1})}}{I_{G(1580\ \mathrm{cm}^{-1})}}.$$

As indicated in Fig. 8, there is a large decrease in R_s (the value of surface R of carbon fibers) during the heat-treatment temperature from 1,800 to 2,800 °C, indicating that the crystal structure of the fibers surface becomes more and more ordered. However, from 1,800 to 2,200 °C, R_c (the value of core R of carbon fibers) shows a small decrease, and above 2,200 °C the R_c keeps at about 1.2. These imply that the effect of heat-treatment temperature to the graphitic degree of carbon fibers core is small after 2,200 °C. The above facts strongly suggest that the fiber's surface is easy to graphitize, while the fiber's core is hard to graphitize. The data denote that increasing heat-treatment temperature made the degrees of skin-core of the carbon fibers increase.

Effect of microstructure on tensile strength

It is well known that the tensile strength of carbon and graphite fibers is greatly influenced by the presence of flaws [19, 20]. Cooper and Mayer [20] showed that for fibers treated at temperatures below 1,000 °C, the failure was essentially brittle and was governed by the presence of stress-raising defects, many of which were actually identified on fracture surfaces. They also suggested that above 1,250 °C the defects in the fibers other than surface flaws are governing the strength, and they interpreted that this may be due to shearing inside the crystallites causing stress concentrations and ultimately the formation of failure cracks. According to Reynolds and Sharp mechanism for tensile failure of carbon fibers [21], the spread of the crack is decided by the crystallite size. When crystallite size increases, the crack is easy to spread abroad reaching critical flaw size. As shown in Fig. 9 a similar result is likewise observed in this article.

R_{sc} is defined as $R_{sc} = R_s/R_c$, which can be used to quantify the degree of skin-core of carbon fibers. The value of R_{sc} is defined between 0 and 1. When R_{sc} is equal to 1, there are no skin-core structures in the carbon fibers, and the carbon fibers are homogenous. When R_{sc} is close to 0, the homogeneous degrees of the carbon fibers decrease, and the skin-core degrees of the carbon fibers increase. Figure 10 illustrates the relationship between tensile strength and R_{sc} of the carbon fibers. It can be seen that the tensile strength increases with increasing R_{sc}, which means that the tensile strength decreases with increasing degree of skin-core structure of the carbon fibers. Thus, a significant decrease in tensile strength with increasing heat-treatment temperature is mainly derived from the increase of crystallite size and the decrease of the degrees of skin-core. The former makes the crack easy to spread abroad reaching critical flaw size and the latter makes the crack easy to form.

Effect of microstructure on tensile modulus

Tensile modulus is the inherent property of carbon fibers and relates to microcrystalline structure. There are three

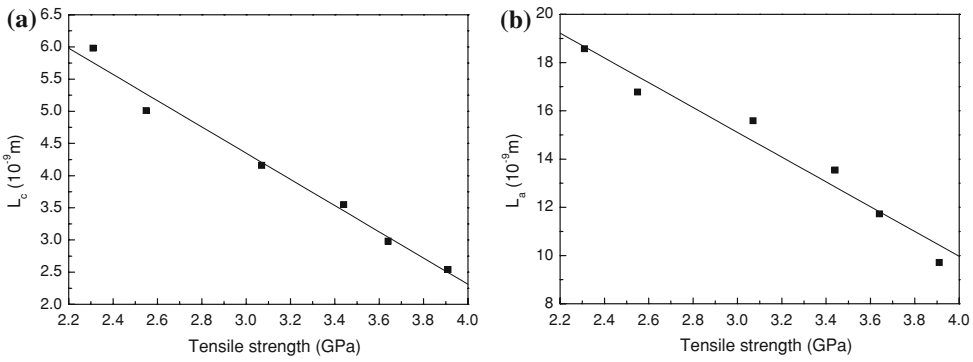

Fig. 9 Correlation between carbon fiber tensile strength and crystallite size L_c (**a**) and L_a (**b**)

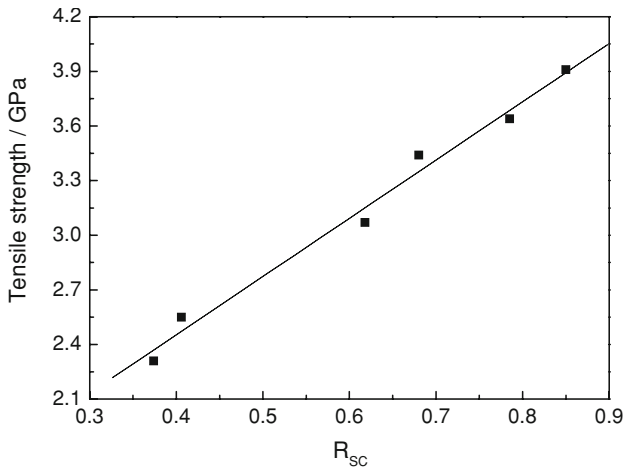

Fig. 10 Correlation between carbon fiber tensile strength and R_{sc}

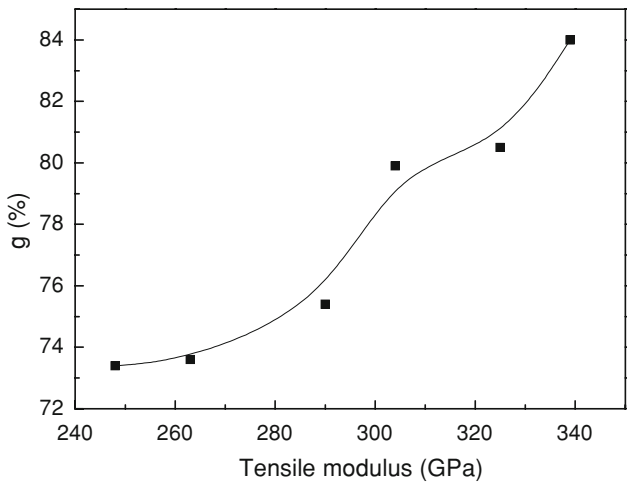

Fig. 11 Effect of the degree of preferred orientation on fibers tensile modulus during graphitization

theoretical models accounting for the relationship between microstructure and tensile modulus, such as uniform stress, uniform strain, and elastic unwrinking. Although different models are used to describe the relationship between microstructure and modulus, it is commonly recognized that a well established correlation exists between preferred orientation (g) and modulus, namely, the bigger g value, the higher modulus.

Figure 11 illustrates the relationship between the degree of preferred orientation of the graphite layer planes and tensile modulus. It can be found that the tensile modulus increases with the increase of the degree of the preferred orientation parameter g. The results are in accordance with the former researchers' viewpoints.

Comparing microstructure parameters gained from X-ray diffraction and Raman analysis, it is evident that apart from the degree of preferred orientation, the crystallite size and the surface graphitization degree in carbon fibers are also important factors on the tensile modulus. Figure 12 shows the changes of crystallite size against the tensile modulus in high heat-treatment temperature

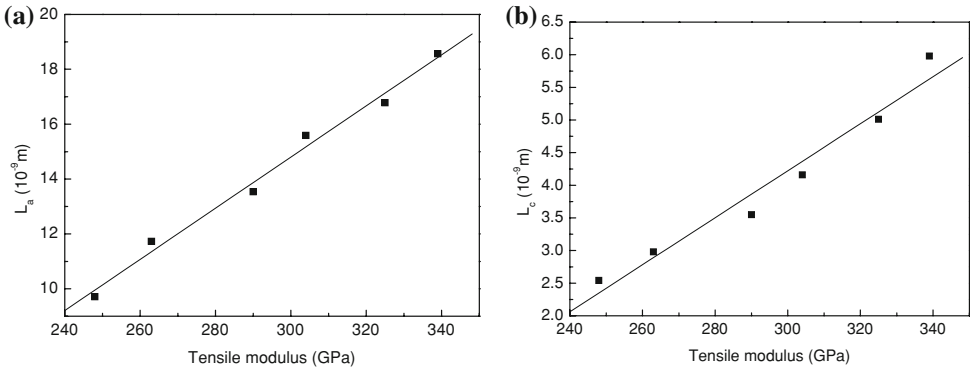

Fig. 12 Effect of crystallite size L_a (**a**) and L_c (**b**) on fibers tensile modulus during graphitization

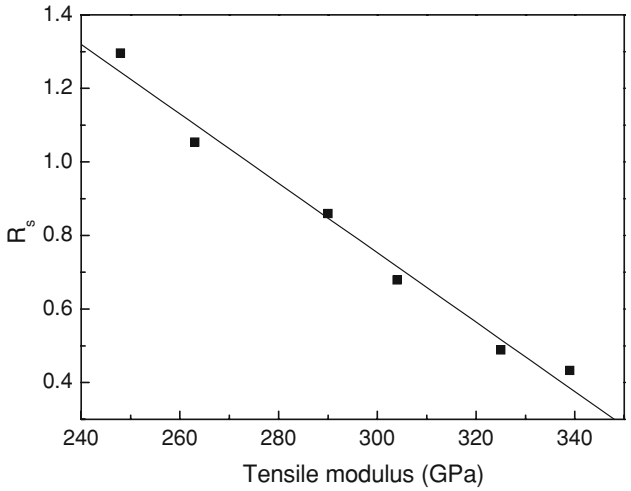

Fig. 13 Effect of R_s on fibers tensile modulus during graphitization

graphitization techniques. It is found that the tensile modulus increases with increasing crystallite size (L_a, L_c). Figure 13 shows the changes of the graphitization degree parameter R_s of carbon fibers surface against the tensile modulus in high heat-treatment temperature graphitization techniques. It can be seen that the tensile modulus increases with the decreasing R_s values, but there is no same relationship between the tensile modulus with the R_c values. It implied that the surface graphitization degree of the carbon fiber has more effect on the tensile modulus than that of the core, and the result is in accordance with Young [22] who said the modulus should be largely determined by the modulus of the larger, stiffer skin of the fiber.

A significant increase in the tensile modulus with increasing heat-treatment temperature mainly comes from the increases in the degree of the preferred orientation, crystallite size (L_a, L_c), and the surface graphitization degree.

Conclusions

In order to evaluate the effect of the microstructure of PAN-based carbon fibers on their tensile strength and tensile modulus under continuous graphitization processing, two analysis methods, Raman spectroscopy and X-ray diffraction, have been used to describe the microstructure of the fibers. The results show that with increasing heat-treatment temperature, both the crystallite size (L_a, L_c) and crystallite preferred orientation degree (g) increase, while the crystallite interlayer spacing (d_{002}) decreases. These imply that the fiber's graphitization degree increases. The values of R_s and R_c both decrease, while R_s decreases more quickly. These imply that the fiber's surface is easy to graphitize, while the fiber's core is hard to graphitize. The degrees of skin-core of the carbon fibers increase with increasing heat-treatment temperature.

It has been demonstrated that the tensile strength is indirectly related to the crystallite size (L_a, L_c) and the degree of skin-core structure, while the tensile modulus not only depended on the preferred orientation, but is also related to the crystallite size (L_a, L_c) and the R_s value. In order to get high property carbon fibers, the crystallite sizes should be controlled within certain range.

Acknowledgements The authors thank Professor He Fu for helpful discussions. The financial support of the National Ministries and Commissions Primary Foundation of China (grant no. 614002) is gratefully acknowledged.

References

1. Huang Y, Young RJ (1995) Carbon 33:97. doi:10.1016/0008-6223(94)00109-D
2. Edie DD (1998) Carbon 36:345. doi:10.1016/S0008-6223(97)00185-1
3. Fizer E (1989) Carbon 27:621. doi:10.1016/0008-6223(89)90197-8
4. Endo M (1988) J Mater Sci 23:598. doi:10.1007/BF01174692
5. Wicks BJ, Coyle RA (1976) J Mater Sci 11:376. doi:10.1007/BF00551449
6. Dieter L, Oskar P, Rennhofer H et al (2007) Carbon 45:2801. doi:10.1016/j.carbon.2007.09.011
7. Sadezky A, Muckenhuber H, Grothe H et al (2005) Carbon 43:1731. doi:10.1016/j.carbon.2005.02.018
8. Montes-Moran MA, Young RJ (2002) Carbon 40:845. doi:10.1016/S0008-6223(01)00212-3
9. Endo M, Kin C, Karaki T et al (1998) Carbon 36:1633. doi:101016/S0008-6223(98)00157-2
10. Melanttis N, Tetlow PL, Galiotis C (1996) J Mater Sci 31:851. doi:10.1007/BF00352882
11. Afanasyeva NI, Jawhari T, Klimenko IV et al (1996) Vib Spectrosc 11:79. doi:10.1016/0924-2031(95)00063-1
12. Young RJ, Lu D, Day RJ et al (1992) J Mater Sci 27:5431. doi:10.1007/BF00541602
13. Cuesta A, Dhamelincout P, Laureyns A et al (1998) J Mater Chem 8:2875. doi:10.1039/a805841e
14. Dresselhaus M, Dresselhaus SG (1981) Adv Phys 30:290. doi:10.1080/00018738100101367
15. Sadezky A, Muckenhuber H, Grothe H et al (2005) Carbon 43:1731. doi:10.1016/j.carbon.2005.02.018
16. Cuesta A, Dhamelincourt P, Laureyns J et al (1994) Carbon 32:1523. doi:10.1016/0008-6223(94)90148-1
17. Wang Y, Alsmeyer DC, McCreery RL (1990) Chem Mater 2:557. doi:10.1021/cm00011a018
18. Al-Jishi R, Dresselhaus G (1982) Phys Rev B 26:4514. doi:10.1103/PhysRevB.26.4514
19. Moreton R, Watt W, Johnson W (1967) Nature 213:690. doi:10.1038/213690a0
20. Cooper GA, Mayer RM (1971) J Mater Sci 6:60. doi:10.1007/BF00550292
21. Johnson DJ (1987) J Phys D Appl Phys 20:287. doi:10.1088/0022-3727/20/3/007
22. Young RJ, Lu D, Day RJ et al (1992) J Mater Sci 27:5431. doi:10.1007/BF00541602